Effect of Carbohydration on the Theranostic Tracer PSMA I&T
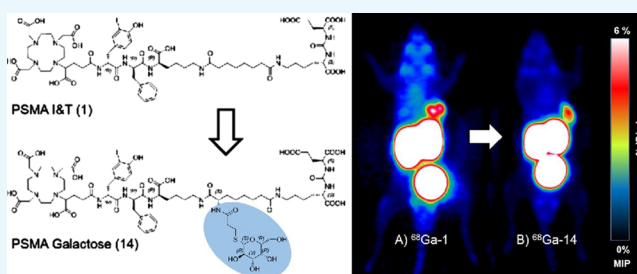
Alexander Schmidt,*[†] Martina Wirtz,[†] Stefanie Felicitas Färber,[†] Theresa Osl,[†] Roswitha Beck,[†] Margret Schottelius,[†] Markus Schwaiger,[‡] and Hans-Jürgen Wester[†]

[†]Pharmaceutical Radiochemistry, Department of Chemistry, Technical University Munich, Walther-Meißner-Street 3, 85748 Garching, Germany

[‡]Department of Nuclear Medicine, Klinikum rechts der Isar, Technical University Munich, Ismaninger Street 22, 81675 Munich, Germany

S Supporting Information

ABSTRACT: To investigate the effect of carbohydrate moieties on the pharmacokinetic profile of prostate-specific membrane antigen (PSMA) inhibitors, carbohydrated derivatives of the established PSMA-targeted radiopharmaceutical PSMA I&T were developed and evaluated. As observed for the reference PSMA I&T, the $^{nat}Ga/^{nat}Lu$ complexes of the respective galactose-, mannose-, and cellobiose-conjugated analogs showed high PSMA affinity. Carbohydration had almost no effect on the lipophilicity, whereas PSMA-mediated internalization was reduced. The specific binding toward human serum albumin (HSA) decreased from 78.6% for [^{nat}Lu]PSMA I&T to 19.9% for the ^{nat}Lu-labeled cellobiose derivative. Compared to [^{68}Ga]PSMA I&T, [^{68}Ga]PSMA galactose displayed lower nonspecific tissue and kidney accumulation but also slightly lower tumor uptake in small-animal positron emission tomography (μPET) imaging. Biodistribution studies confirmed reduced unspecific uptake in nontarget tissue and decreased renal accumulation of the metabolically stable [^{68}Ga]PSMA galactose derivative, resulting in overall improved tumor-to-tissue ratios. However, carbohydration has no significant beneficial in vivo effect on the targeting performance of PSMA I&T. Nevertheless, carbohydration expands the repertoire of feasible modifications within the linker area and might be a valuable tool for the future development of PSMA inhibitors with decreased kidney uptake.

INTRODUCTION

Prostate-specific membrane antigen (PSMA), a type II transmembrane protein, was discovered to be considerably overexpressed on most prostate cancer (PCa) cells and to correlate with its expression level the more advanced the disease becomes.[1−4] The exceptional target characteristics of PSMA enabled the development of radiolabeled PSMA inhibitors and antibodies for imaging and endoradiotherapy of PCa.[5−11] Although [^{68}Ga]PSMA-HBED-CC (Figure 1) is the most widely studied PSMA agent for clinical PCa-PET imaging, [^{177}Lu]PSMA I&T and [$^{177}Lu/^{225}Ac$]PSMA-617 (Figure 1) are currently used for endoradiotherapy of metastatic castration-resistant prostate cancer (mCRPC).[12−15]

Radioligand therapy with [^{177}Lu]PSMA I&T is well tolerated and has been demonstrated to be an efficient treatment option in advanced mCRPCa. No renal toxicity was observed, and only a few cases of heavily pretreated patients developed grade 3 or 4 hematological toxicity, thus confirming the safety of [^{177}Lu]PSMA I&T.[13] Dosimetric studies revealed that tumor lesions received the highest radiation doses (3.3 mGy/MBq), followed by the parotid glands (1.3 mGy/MBq) and the kidneys (0.8 mGy/MBq), which shows the parotid glands and the kidneys to be dose limiting.[14] On the basis of the experience gained so far, patients have already been treated

with up to 10 cycles of ^{177}Lu-labeled PSMA inhibitors without significant side effects, which relativizes the focus on the kidney as a "dose-limiting organ." However, a reduction of unwanted tissue uptake is generally recommended during the drug development of radiolabeled tracers to reduce the possible adverse effects.

A well-established approach to reduce unwanted renal accumulation of peptidic tracers and to enhance their in vivo elimination is the introduction of carbohydrate moieties.[16−19] Several investigations have shown that the conjugation of a carbohydrate can significantly alter the in vivo and in vitro parameter and thus, for instance, reduce the kidney uptake, reduce unspecific tissue binding, or improve the overall biodistribution profile of the radiolabeled ligand. Therefore, with the intention to develop a PSMA inhibitor with low kidney uptake, we used PSMA I&T as a starting point and introduced a free amine group within the suberic acid spacer for rapid derivatization. After the conjugation of three different thio-linked carbohydrate moieties (two monosaccharides: galactose, mannose; one diglycoside: cellobiose), we evaluated
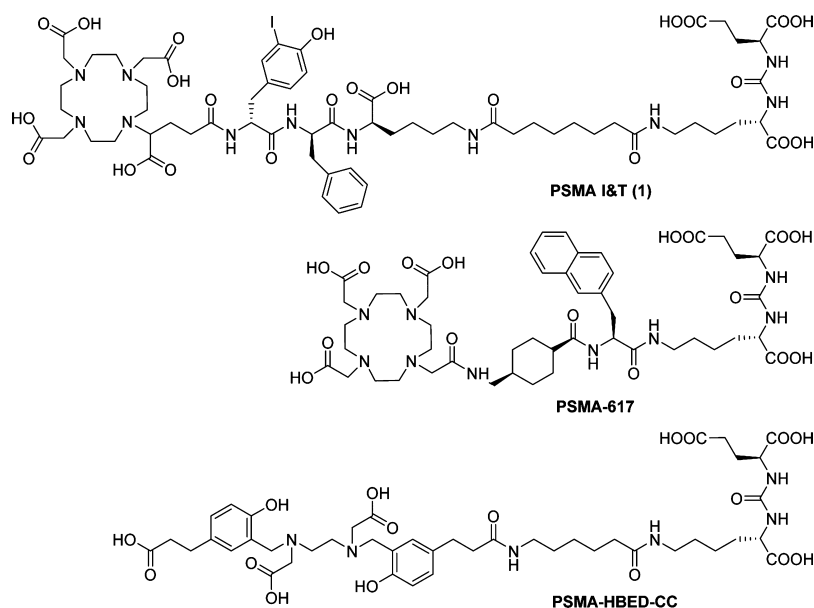
Figure 1. Structures of PSMA I&T (**1**), PSMA-617, and PSMA-HBED-CC.

the novel carbohydrated compounds with respect to the most important parameters, such as affinity, internalization, and lipophilicity. Additionally, we investigated the effect of carbohydration on albumin binding. On the basis of the in vitro data, [^{68}Ga]PSMA galactose was selected for a further comparative in vivo evaluation with [^{68}Ga]PSMA I&T in CB-17 severe combined immunodeficiency (SCID) mice.

RESULTS

Synthesis. The introduction of thioglycosides into the linker region was achieved using Fmoc-L-Asu(O*t*Bu)-OH as the starting point (Figure 2). The protection of the free carboxylic group and the concomitant removal of the *t*Bu protecting group with trifluoroacetic acid yielded 90% of **4** after RP-HPLC purification. Coupling of **4** with the binding motif **1** and subsequent benzyl deprotection resulted in 92% yield of **7**. DOTAGA-(I-y)fk was synthesized as previously published and condensed with **7** to establish **9** without further purification.[20] After Fmoc and subsequent *t*Bu deprotection, **10** was obtained in 41% yield after RP-HPLC purification. Condensation of **10** with the PfpOH-activated thioglycosides **11**, **12**, and **13** facilitated the final carbohydrated derivatives **14**, **15**, and **16** in yields of 3 to 10% after deacetylation and purification via RP-HPLC.

Radiochemistry. *^{68}Ga Labeling.* The synthesis of the ^{68}Ga-labeled PSMA inhibitors (e.g., 5.0 nmol) was achieved within 15 min after the start of the radiosynthesis and resulted in specific activities ranging from 35 to 53 GBq/μmol after cartridge purification. The radiochemical purity for all compounds was ≥97%.

^{177}Lu Labeling. With minor modifications to the previously published protocol, ^{177}Lu labeling was accomplished with radiochemical purities ≥98% and specific activities ranging from 10 to 53 GBq/μmol.[21]

^{125}I Labeling. ([^{125}I]I-BA)KuE, the reference ligand for all in vitro studies, was synthesized according to procedures mentioned in the literature.[20,22−24] Destannylation of the precursor **17** was achieved with [^{125}I]NaI and peracetic acid within 10 min at room temperature. Consecutive cartridge purification, *t*Bu deprotection with trifluoroacetic acid, and

purification via RP-HPLC resulted in the final product ([^{125}I]I-BA)KuE with a radiochemical purity ≥99% and a radiochemical yield of 41 ± 10%.

PSMA Affinity (IC$_{50}$). Binding to PSMA was determined using LNCaP human prostate cancer cells in a competitive binding assay with the ^{nat}Ga or ^{nat}Lu analogs of **14**, **15**, and **16** and ([^{125}I]I-BA)KuE (*c* = 0.2 nM) as the radioligand. For comparison, the IC$_{50}$ values of PSMA I&T (**1**) were taken from a previous publication,[7] in which the same binding assay was performed. The results given in Table 1 show that the affinities of the monosaccharide derivatives **14** and **15** were not significantly higher compared to that of the reference PSMA I&T (**1**). The introduction of the disaccharide cellobiose (**16**) lowered the affinity, also not significantly. The different stereochemistry of the carbohydrates used in **14** and **15** showed minimal effect on the binding affinity.

Internalization. LNCaP cells were used to investigate the cell surface binding and internalization of the ^{68}Ga- and ^{177}Lu-labeled compounds **14**, **15**, and **16**. The cell surface-bound fraction after 60 min incubation ranged from 0.6 to 1.0%, whereas the internalized fraction displayed values from 1.3% for ^{68}Ga-**16** to 11.3% for ^{177}Lu-**14** for the total applied activity. Normalized to the uptake of ([^{125}I]I-BA)KuE, the results in Table 1 show that all carbohydrated compounds exhibited significantly lower values in comparison to **1** and the ^{68}Ga-labeled compounds internalized less than the ^{177}Lu-analogs. Differences in the stereochemistry of **14** and **15** resulted in slightly higher internalization of the galactose derivative.

Human Serum Albumin Binding. Albumin binding was determined using a human serum albumin (HSA) column connected to an HPLC system.[25,26] Column calibration was always performed prior to the analysis of the ^{nat}Ga- and ^{nat}Lu-labeled PSMA inhibitors and resulted in a coefficient of determination (r^2) > 92% in all experiments. The results given in Table 1 display a range of HSA binding from 6.9% for ^{nat}Ga-**15** to 78.6% for ^{nat}Lu-**1**. Comparing **14** and **15**, stereochemistry had only a marginal influence on the albumin-binding values. Overall, carbohydration reduced the albumin binding in comparison to the reference ligand **1**.
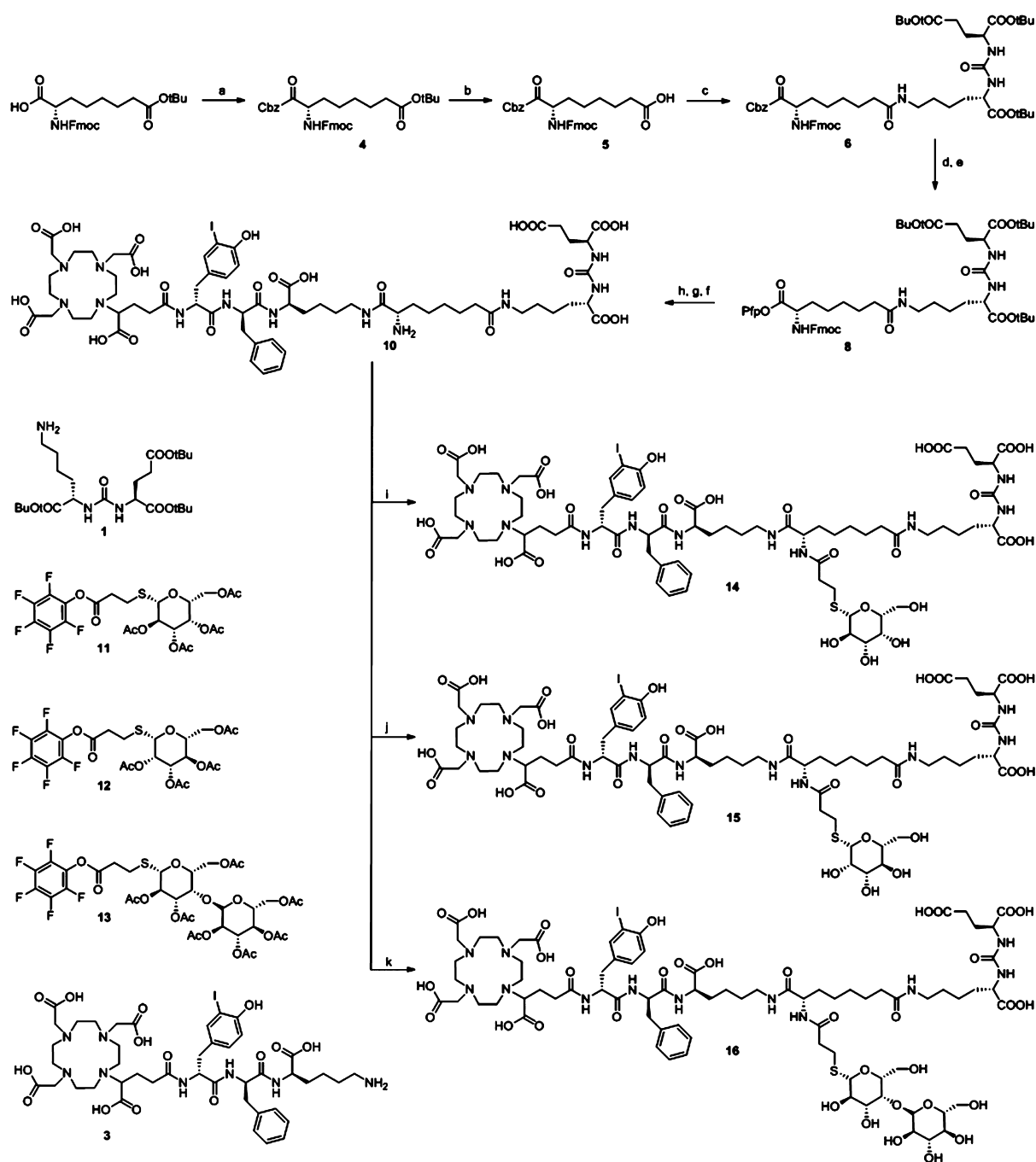
Figure 2. Synthesis of the carbohydrated PSMA inhibitors **14**, **15**, and **16**. (a) HOAt, HATU, DIPEA, benzyl alcohol, [DMF]; (b) 95% TFA, 5% DCM; (c) **1**, HOBt, TBTU, DIPEA, [DMF]; (d) Pd/C (10%), H$_2$, [EtOH]; (e) DIC, PfpOH, pyridine, [DMF]; (f) **3**, DIPEA, [DMF]; (g) 20% piperidine in DMF, [DMF]; (h) TFA; (i) **11**, DIPEA, [DMF]; (j) **12**, DIPEA, [DMF]; (k) **13**, DIPEA, [DMF].

Lipophilicity. For all compounds, the respective ^{177}Lu-labeled analogs were more lipophilic than the ^{68}Ga-labeled counterparts. The introduction of a sugar moiety altered hydrophilicity only to a negligible extent and not significant with ^{68}Ga-**14** being the most hydrophilic carbohydrated PSMA inhibitor displaying a log P value of -4.15 ± 0.07. Data for ^{68}Ga- and ^{177}Lu-**1** were obtained from a previously published report and are added in Table 1 for comparison.[27]

Metabolic Stability. The in vivo stability of [^{177}Lu]PSMA galactose was investigated in a healthy mouse 60 min postinjection (p.i.). Figure 3 shows the extracted samples from the urine, blood, and kidneys, which were analyzed using radio-HPLC. The extraction rate of ^{177}Lu-**14** using 2-PMPA as a competitor was ≥31% per investigated tissue (≥0.5 MBq) and enabled sufficient signal intensity. ^{177}Lu-**14** was found to be stable over 60 min in all analyzed fractions.

μPET Imaging and Biodistribution. ^{68}Ga-**14** exhibited lower uptake in non-PSMA-expressing tissue but also reduced tumor accumulation compared to ^{68}Ga-**1** (3.7 ± 0.5% ID/mL vs 5.8 ± 0.3% ID/mL; 85 min p.i.; Figures 4 and 5). The specificity of the PSMA-mediated tissue uptake of ^{68}Ga-**14** in the kidneys and the xenograft was confirmed by the coinjection of 2-PMPA (8 mg/kg), which reduced the uptake in these tissues to the background level.

Table 1. PSMA Binding Affinities (IC_{50}), Internalization (%), Lipophilicity (log P), and HSA Binding of the Investigated Compounds[a]

PSMA inhibitor		IC_{50} [nM]	internalization [%]	log P	HSA [%]
[nat/68Ga]PSMA I&T	(nat/68Ga-**1**)	9.4 ± 2.9	59.2 ± 1.7	−4.31 ± 0.32	52.0
[nat/177Lu]PSMA I&T	(nat/177Lu-**1**)	7.9 ± 2.4	75.5 ± 1.6	−4.12 ± 0.10	78.6
[nat/68Ga]PSMA galactose	(nat/68Ga-**14**)	7.9 ± 3.9*	18.7 ± 4.1**	−4.15 ± 0.07*	7.7**
[nat/177Lu]PSMA galactose	(nat/177Lu-**14**)	5.8 ± 0.6*	60.2 ± 2.8**	−3.95 ± 0.12*	23.3**
[nat/68Ga]PSMA mannose	(nat/68Ga-**15**)	7.1 ± 0.3*	8.4 ± 0.2**	−4.01 ± 0.08*	7.6**
[nat/177Lu]PSMA mannose	(nat/177Lu-**15**)	5.9 ± 0.5*	35.3 ± 2.9**	−3.85 ± 0.04**	25.1**
[nat/68Ga]PSMA cellobiose	(nat/68Ga-**16**)	10.8 ± 1.7*	4.0 ± 0.6**		6.9**
[nat/177Lu]PSMA cellobiose	(nat/177Lu-**16**)	12.5 ± 2.3*	22.3 ± 1.2**	−4.04 ± 0.10*	19.9**

[a]Binding assays (IC_{50}) were performed using LNCaP cells (150 000/well) and ([125I]I-BA)KuE (c = 0.2 nM) as the radioligand. Cells were incubated in HBSS (1% BSA) at 4 °C for 1 h. Internalization values were corrected for unspecific binding and normalized to the reference ([125I]I-BA)-KuE (c = 0.2 nM for 68Ga and 0.5 nM for 177Lu compounds; 37 °C, 1 h, 125 000 cells/well, PLL-coated plates). Data for binding (IC_{50}) and internalization are expressed as mean ± SD (n = 3). Data are expressed as mean ± SD (n = 6) for log P. HSA binding (%) was determined via HPLC and nonlinear regression calibration using the t_R of the natGa- and natLu-labeled PSMA inhibitors.* = P > 0.05; ** = P < 0.05.

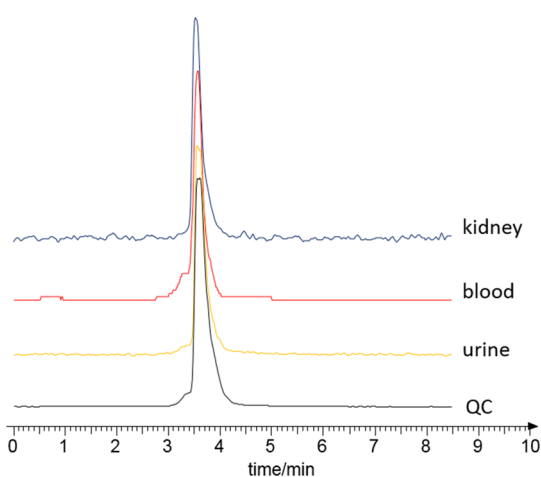**Figure 3.** Metabolite study of 177Lu-**14**. Radio-HPLC analyses of quality control (QC) and extracts from homogenized organs and body fluids from a male CB-17 SCID mouse (60 min p.i., 25 MBq 177Lu-**14**). Chromolith column, binary gradient, flow rate 3 mL/min, 3% MeCN to 95% MeCN in 6 min, 95% MeCN for 3 min.
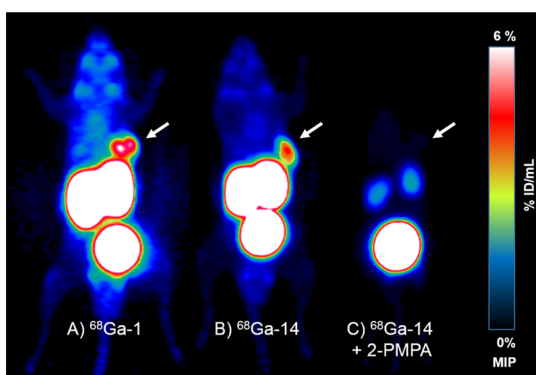

Figure 4. Maximum intensity projections (MIPs) of μPET scans in LNCaP xenograft-bearing mice. Dynamic MIP (summed up frames 1 to 1.5 h p.i.) of (A) 7.0 MBq 68Ga-**1** (PSMA I&T) and (B) 12 MBq 68Ga-**14** (0.15−0.20 nmol of peptide, respectively). (C) Static MIP (1 h p.i. for 15 min) of 68Ga-**14** + PMPA coinjection (8 mg/kg). Arrow indicates LNCaP tumor xenograft uptake in (A,B) or blockade of tumor uptake in (C).

The logarithmic plot of the time−activity curves (TACs) in Figure 5 shows a linear decrease of 68Ga-**14** from the heart and

muscle tissue. Direct comparison of 68Ga-**1** and 68Ga-**14** in the linear TAC in Figure 5 illustrates the reduced tumor uptake of 68Ga-**14** compared to 68Ga-**1** (3.7 ± 0.5 vs 5.8 ± 0.3% ID/mL, 68Ga-**14** and 68Ga-**1**, 85 min p.i.). However, it also shows that 68Ga-**14** accumulates to a lower extent in the kidneys with an earlier onset of elimination (43.1 ± 2.2 vs 74.6 ± 3.6% ID/mL, 68Ga-**14** and 68Ga-**1**, 85 min p.i.).

Except for the blood value 1 h p.i., 68Ga-**14** showed decreased tissue uptake compared to 68Ga-**1** (Figure 6). Reduced accumulation of 68Ga-**14** was further seen in the spleen, kidneys, and tumor (3.86 ± 1.32 vs 4.37 ± 0.64% ID/g uptake in tumor, 68Ga-**14** and 68Ga-**1**, 1 h p.i.). Progressive clearance of 68Ga-**14** from the kidneys and other tissues was visible up to 3 h after injection, whereas tumor uptake remained constant (3.85 ± 0.54% ID/g, 3 h p.i.).

A direct comparison of the tumor-to-tissue ratios of 68Ga-**1** and 68Ga-**14** at 1 h p.i. in Figure 7 shows slightly increased ratios for the carbohydrated derivative 68Ga-**14** compared to 68Ga-**1**. The reduced kidney and tumor uptake of 68Ga-**14** resulted in similar tumor-to-kidney ratios for both tracers (0.07 vs 0.06, 68Ga-**14** and 68Ga-**1**, respectively).

■ DISCUSSION

The recent development of PSMA ligands has resulted in highly specific radiolabeled agents for radioguided surgery, endoradiotherapy, and imaging of PCa.[6,7,27−31] One of the widespread clinically used compounds is PSMA I&T, a ligand recently developed by our group.[32] Although no significant side effects have been observed so far, possible adverse reactions due to unwanted uptake of [177Lu]PSMA I&T (**1**) in the kidneys and salivary glands might impact the cumulative radioactivity dose, which can be administered for endoradiotherapy.[14]

Several investigations by our group have demonstrated that carbohydration is a valuable tool to optimize the pharmacokinetics of compounds showing unfavorable in vivo distribution patterns.[17,19,33−37] It was also shown that depending on the utilized sugar moiety, the adjustment of renal drug handling is feasible.[34,38,39] Therefore, in this study, we have aimed at developing carbohydrated PSMA inhibitors with preserved bioactivity to investigate the effect of carbohydration on the in vivo profile of the theranostic tracer PSMA I&T.

The conjugation of the thioglycosides of galactose and mannose to the suberic acid linker unit between the binding motif and the peptidic scaffold surprisingly resulted in slightly
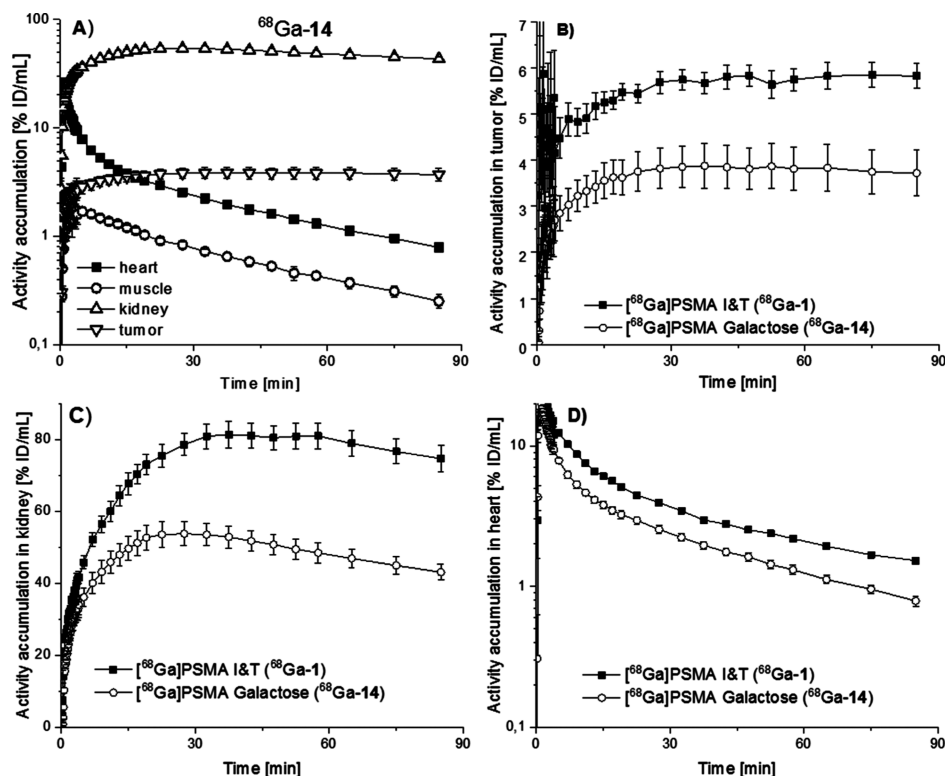
Figure 5. Time−activity curves (logarithmic and linear plot) in % ID/mL. (A) [68]Ga-**14** in selected organs. Comparison of [68]Ga-**14** vs [68]Ga-**1** (PSMA I&T) in (B) tumor, (C) kidney uptake, and (D) blood pool (heart) uptake. Data obtained from μPET imaging in LNCaP xenograft-bearing CB-17 SCID mice.
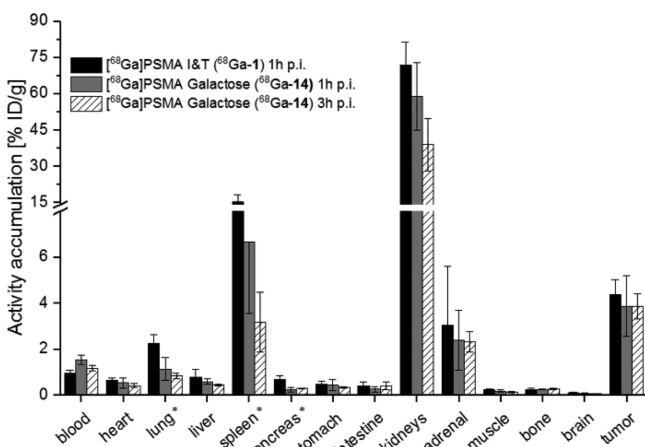

Figure 6. Biodistribution data (in % ID/g). Biodistribution in healthy CB-17 SCID mice for [68]Ga-**1** at 1 h p.i. and in LNCaP tumor-xenograft bearing CB-17 SCID mice for [68]Ga-**14** at 1 and 3 h p.i. ($n = 4$). * = $P < 0.05$.
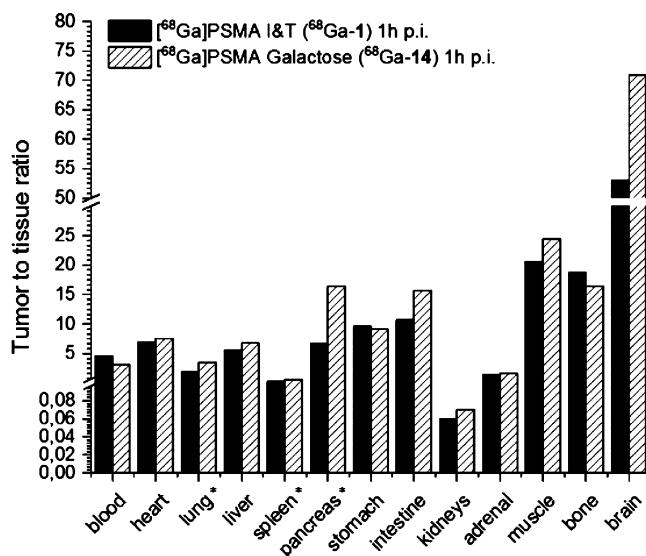

Figure 7. Tumor-to-tissue ratios of [68]Ga-**1** and [68]Ga-**14** in selected organs at 1 h p.i. * = $P < 0.05$.

higher affinities than in the parent compound **1** (Table 1) and demonstrated the unexpected tolerability of PSMA I&T to incorporate bulky hydrophilic moieties in close proximity to the S1-binding pocket.

These results are, however, in contrast to a recently published report by Bouvet et al.[40] Their [^{18}F]FDG-based PSMA ligand exhibited only moderate binding to PSMA, whereas every other compound, modified with an aromatic residue, was found to have a significantly higher affinity.[40] The hydrophobic pocket adjacent to the S1-binding site of PSMA, which is amenable for π-stacking and π-cationic interactions

with hydrophobic motifs, explains this observation because no such interactions are possible with a carbohydrate, such as [^{18}F]FDG.[41] Yet, PSMA I&T was developed with the intention to interact in a bidentate mode with the binding cavity of PSMA and the remote arene-binding site through the peptidic spacer and, therefore, probably compensates the potentially negative steric requirement of the sugar moieties. Moreover, the tunnel region of PSMA was reported to be partially tolerant toward structural modification,[42,43] which might explain the

fact that even the disaccharide analog ^{nat}Lu-**16** exhibited a reasonably high affinity (IC$_{50}$ = 12.5 ± 2.3 nM).

Although lipophilicity was only negligibly affected and resulted in log P values $\leq$ −3.85 for all investigated compounds, carbohydration had a considerable and significant impact on tracer internalization. In concordance with previous reports,[7,20] the ^{68}Ga-labeled compounds exhibited constantly lower intracellular activity than the respective ^{177}Lu-labeled analogs, and notably, the lowest internalization efficiency of only 4.0 ± 0.6% [relative to the reference ([^{125}I]I-BA)KuE] measured in this study was observed for ^{68}Ga-**16**. This observation might be explained by either the hexa- or the heptadentate complexation of gallium and lutetium, respectively, and thus the resulting additional free carboxylic group in the case of gallium, which might impede the in vitro interactions, which are necessary for internalization. A detailed structure−activity relationship about the mechanism of internalization after ligand binding to PSMA has not been reported so far. However, the general mechanism has been shown to rely on endocytosis via clathrin-coated pits.[1,44,45] Our data suggest that sterically demanding carbohydrates at this conjugation side of the molecule affect the internalization process of PSMA and display a low tolerance for bulky hydrophilic moieties within the tunnel region. Further, an additionally negative charge in the chelator region reduces the internalization rate. These results are in agreement with the findings of Liu et al., who stated that the binding of the inhibitor induces a conformational change in PSMA, which either interferes with or contributes to the interaction of PSMA's cytoplasmatic tail with clathrin and the clathrin adaptor protein-2.[46]

Analogous to the decreased internalization rate, binding to human albumin declined significantly. After carbohydration, the value of ^{nat}Ga-**14** is more than six times lower compared to that of ^{nat}Ga-**1** (7.7% vs 48.7%; 1 h), and the same effect was observed for every other tested carbohydrated derivative in this study (Table 1). It is known that human albumin binds especially to molecules with lipophilic structures and negative charges in close proximity. It is therefore reasonable that the carbohydrates interfere with the interaction of albumin with the otherwise lipophilic suberic acid structure of the parent ligand PSMA I&T. Because of the positive results observed by Suzuki et al.[34] regarding the reduction of kidney uptake after conjugation to galactose, ligand **14** was used for further investigation.

Delayed plasma clearance is especially interesting for possible therapeutic applications. Increased tracer activity in the blood pool leads to higher tracer availability and thus increases the probability of the ligand to bind the target and to be potentially internalized. This can be achieved, for example, through the introduction of an albumin-binding tag, as demonstrated for radiolabeled folic acid compounds and recently for PSMA ligands.[47−49] In contrast, low plasma protein binding might be beneficial in terms of the low background activity for PET imaging quality with earlier acquisition after intravenous injection and reduced radiation doses during endoradiotherapy because radiolabeled PSMA tracers are retained at the target side. A higher unbound fraction in the blood pool should result in a faster plasma clearance, if the renal clearance into the bladder is considered as the primary elimination process.[50,51] This situation was clearly demonstrated in the dynamic μPET imaging and, compared to [^{68}Ga]PSMA I&T, reduced background activity

and faster plasma clearance of ^{68}Ga-**14** were visible (Figures 5 and 6).

Yet, in contrast to the dynamic PET study, the biodistribution study showed an elevated blood activity level for the carbohydrated compound ^{68}Ga-**14** compared to ^{68}Ga-**1**. A possible explanation, besides the limited number of PET studies, is the possible metabolite formation. Nevertheless, no substantial metabolite formation of ^{177}Lu-**14** after 60 min p.i. was observed (Figure 3). Hence, the elevated blood uptake of ^{68}Ga-**14** has so far not been attributable to a specific effect but rather explainable through the reduced unspecific uptake in other tissue compartments, as shown in the biodistribution study. Except for the blood value at 1 h p.i. (1.53% ID/g vs 0.96% ID/g, ^{68}Ga-**14** vs ^{68}Ga-**1**, respectively), equal (bone, pancreas) or lower uptake in all other investigated tissues was visible for ^{68}Ga-**14** compared to ^{68}Ga-**1** (Figures 7 and 6). Yet, only the ligand uptake in the lung, spleen, and pancreas is significantly lower compared to the reference PSMA I&T (P < 0.05). Taking the superior in vitro parameter of $^{nat/177}$Lu-**14** compared to the $^{nat/68}$Ga-labeled derivative into account, a biodistribution study with ^{177}Lu-**14** should result in a higher tumor uptake because of the higher affinity and internalization. However, the increased plasma protein binding would also lead to a higher blood uptake and therefore probably level out the tumor-to-tissue ratios.

A similar observation regarding blood uptake was reported by Susaki et al.[39] All carbohydrated vasopressin derivatives in their study displayed a higher blood level in comparison to the non-carbohydrated compound. Likewise, they contributed this effect to decreased unspecific tissue uptake and thus the resulting elevated plasma levels. Suzuki et al. showed additionally that derivatization with galactose reduced binding to microsomal kidney and liver fractions.[34]

Several groups emphasize the importance of the internalization to increase the tumor accumulation of PSMA ligands.[20,44,52,53] The lower internalization of ^{68}Ga-**14**, therefore, probably caused the slightly reduced tumor uptake compared to ^{68}Ga-**1** (3.85 ± 0.54 vs 4.37 ± 0.64% ID/g, 1 h p.i.). In this respect, reduction of the internalization upon carbohydration may be considered as a drawback, and other carbohydrate moieties should be evaluated to investigate if distinct glycosides or other positions within the molecule are able to increase the internalization while maintaining high affinity. However, recent reports about the superiority of radiolabeled somatostatin-2 (sst$_2$) antagonists compared to sst$_2$ agonists and other tracer groups have led to reconsideration of the importance of the parameter internalization.[54−57] It is so far not clear if a "real" antagonistic PSMA inhibitor without internalization would perform similarly to the sst$_2$ antagonists. Hence, further studies regarding the internalization mechanism of PSMA and its importance are needed.

■ CONCLUSIONS

Carbohydration altered the in vitro properties of PSMA I&T, but without significant benefit in vivo. Although high affinity was maintained, the internalization rate and especially the HSA binding dropped considerably after the introduction of a carbohydrate moiety. The derivatives **14**, **15**, and **16** demonstrate the possibility to conjugate highly hydrophilic bulky carbohydrates to PSMA I&T-based structures and thus increase the repertoire of pharmacokinetic modifications for further development of PSMA ligands, especially for compounds suffering from high lipophilicity.

MATERIALS AND METHODS

General. The general information about the used materials, methods, and synthesis of the carbohydrated derivatives **14–16** and the nonradioactive Ga- and Lu-labeled references [^{nat}Ga/^{nat}Lu]**14–16** together with the synthesis of the precursor used for ^{125}I labeling to obtain the radioligand ([^{125}I]I-BA)KuE for the in vitro experiments is found in the Supporting Information. All analytical data regarding ESI-MS and RP-HPLC for the synthesized compound **14–16** are also found in the Supporting Information.

Radiolabeling. *^{68}Ga Labeling.* For in vitro and in vivo studies, the ^{68}Ga-labeled compounds were prepared using a fully automated system employing a ^{68}Ge/^{68}Ga generator (iThemba Labs, South Africa) connected to GallElut+ system (SCINTOMICS GmbH, Germany). The radiolabeling was already described in previous reports.[20,58,59] The experimental details are provided in the Supporting Information.

^{177}Lu Labeling. The ^{177}Lu-labeled compounds were prepared as previously described with minor modifications and used without further purification.[21] In short, into a 500 μL reaction tube, NH$_4$OAc buffer (10 μL, 1.0 M, pH = 5.9), 0.75–1.0 nmol tracer (7.5–10 μL, trace-pure water, Merck, Darmstadt, Germany), and 10 to 40 MBq ^{177}LuCl$_3$ were added (specific activity (A_S) > 3000 GBq/mg, 740 MBq/mL, 0.04 M HCl, ITG, Garching, Germany), and the reaction mixture was filled up to 100 μL with trace-pure water. The reaction mixture was heated for 30 min at 95 °C and the radiochemical purity was determined using radio-TLC.

^{125}I Labeling. The radioiodinated reference ligand ([^{125}I]I-BA)KuE was synthesized in accordance with a previously published method and fully described in the Supporting Information.[20]

In Vitro Assays. *Cell Culture.* PSMA-positive LNCAP cells (CLS: 300265; Cell Lines Service GmbH) were cultivated in Dulbecco modified Eagle medium/nutrition mixture F-12 (1:1) (DMEM-F12, Biochrom) supplemented with 10% fetal calf serum (Biochrom) and kept at 37 °C in a humidified 5% CO$_2$ atmosphere. One day (24 ± 2 h) prior to all in vitro experiments with LNCaP cells, the cultivated cells were harvested using a mixture of trypsin/ethylendiaminetetraacetate (0.05%/0.02%) in phosphate-buffered saline (PBS) and centrifuged. After centrifugation, the supernatant was disposed and the cell pellet was resuspended in culture medium. Afterward, cells were counted with a hemocytometer (Neubauer) and seeded in 24-well plates. IC$_{50}$ values were determined by transferring 150 000 cells/mL per well into 24-well plates, whereas internalization was assessed by transferring 125 000 cells/mL into 24-well PLL-coated plates.

Determination of IC$_{50}$ and Internalization. Detailed information regarding affinity and internalization experiments is provided in the Supporting Information.[20]

Summary. The determination of binding affinity (IC$_{50}$) was performed using LNCaP cells at 4 °C with ([^{125}I]I-BA)KuE as the radioligand and the respective ^{nat}Ga- and ^{nat}Lu-PSMA inhibitors. After incubation for 1 h, the cell-bound and free activity were separated and quantified in a γ-counter. All experiments were performed in triplicate.

For internalization experiments, the ^{68}Ga- and ^{177}Lu-labeled compounds were incubated for 1 h at 37 °C. Afterward, the experiments were stopped through placing the 24-well plate on ice for 5 min. After separation of the supernatant (unbound fraction), the cell-surface-bound activity was removed through

incubation with a 2-PMPA solution for 5 min. Finally, the internalized activity was gained through lysis with 1.0 M NaOH solution. All fractions were collected and quantified in a γ-counter, and the uptake was calculated relative to the uptake of ([^{125}I]I-BA)KuE as the reference. All experiments were performed in triplicate.

HSA Binding. HSA binding experiments were performed, as previously described, by the application of an HSA column connected to an HPLC system with a UV–vis detector.[25] The mobile phase consisted of a binary gradient system with a constant flow rate of 0.5 mL/min. Mobile phase A consisted of an ammonium acetate solution (50 mM, pH 6.9); mobile phase B was 2-propanol (HPLC grade, VWR, Germany). The gradient of mobile phase A was 100% from 0 to 3 min and from 3 min to the end of each run; mobile phase B was set at 20%. On each experimental day, the column was calibrated with nine reference substances to confirm the performance and to conduct the nonlinear regression. Afterward, the PSMA inhibitors with unknown HSA binding were measured. All substances were dissolved in a 0.5 mg/mL concentration and 5–10 μL was injected for each run. Further information is provided in the Supporting Information.

Lipophilicity. The log P values were determined, as previously described, using the shake flask method.[20]

Statistical analysis was performed for affinity, internalization, and lipophilicity using a t-test (Microsoft Excel software). All analyses were two-tailed and considered as type 3 (two-sample unequal variance). A P value of less than 0.05 was considered statistically significant.

In Vivo Experiments. All animal experiments were carried out in accordance with the general animal welfare regulations in Germany (Deutsches Tierschutzgesetz, approval #55.2-1-54-2532-71-13). For the xenograft tumor model, LNCaP cells (approximately 10^7 cells) were suspended in a serum-free DMEM-F12 medium and Matrigel (BD Biosciences, Germany) (1:1) and inoculated onto the right shoulder of 6 to 8 weeks old male CB-17 SCID mice (Charles River Laboratories, Sulzfeld, Germany). Animals were used for in vivo studies after the tumor size reached 4–8 mm in diameter.

Metabolic Stability. [^{177}Lu]PSMA galactose (^{177}Lu-**14**; 25 MBq) was injected into the tail vein of a healthy CB-17 SCID mouse (n = 1), which was sacrificed after 60 min. Samples of the urine and blood were immediately taken. Kidneys were frozen with liquid nitrogen, homogenized, and extracted with 2-PMPA solution (500 μL, 400 μM in PBS). After centrifugation at 15 000g for 5 min, the suspension was ultrafiltrated and analyzed by radio-HPLC. The blood sample was centrifuged at 6000g for 5 min to obtain the plasma. To remove the proteins from the plasma, ice-cold MeCN was added to the sample, which was later incubated for 10 min at 4 °C. After concomitant centrifugation and ultrafiltration, the sample was analyzed by radio-HPLC. The urine sample was used without any further preparation.

μPET Imaging. Imaging experiments were conducted using a Siemens Inveon small-animal PET. The resulting data were analyzed by the associated Inveon Research Workplace software. Mice were anaesthetized with isoflurane, and the compounds [^{68}Ga]PSMA I&T (^{68}Ga-**1**) and [^{68}Ga]PSMA galactose (^{68}Ga-**14**) (0.2 nmol, 7.0 and 12 MBq, respectively) were injected via the tail vein (n = 1). Dynamic imaging was carried out after on-bed injection for 90 min. The static blockade image was obtained after 1 h p.i. with 15 min acquisition time. Blockade was performed by coinjection of 8

mg/kg of 2-PMPA. All images were reconstructed using an OSEM 3D algorithm without scanner and attenuation correction.

Biodistribution. Approximately 10.0 to 11.0 MBq (ca. 0.2 nmol) of [^{68}Ga]PSMA galactose (^{68}Ga-**14**) and 6.3−7.0 MBq (ca. 0.2 nmol) of [^{68}Ga]PSMA I&T (^{68}Ga-**1**) were injected into the tail vein of LNCaP tumor-bearing male CB-17 SCID mice (*n* = 4), which were sacrificed after either 1 h p.i. (^{68}Ga-**1** and ^{68}Ga-**14**) or 3 h p.i. (^{68}Ga-**14**). Selected organs were removed, weighted, and measured in a γ-counter. Statistical analysis for the biodistribution study was performed using a *t*-test (Microsoft Excel software). All analyses were two-tailed and considered as type 3 (two-sample unequal variance). A *P* value of less than 0.05 was considered statistically significant.

ASSOCIATED CONTENT

Ⓢ Supporting Information

The Supporting Information is available free of charge on the ACS Publications website at DOI: 10.1021/acsome-ga.8b00790.

> Additional details on experimental methods, synthesis, radiolabeling methods, and in vitro experiments (PDF)

AUTHOR INFORMATION

Corresponding Author
*E-mail: alex030488@gmail.com (A.S.).

ORCID ⓘ
Alexander Schmidt: 0000-0002-5445-3852

Notes
The authors declare the following competing financial interest(s): The carbohydrated ligands are part of a European patent application.

ACKNOWLEDGMENTS

ABBREVIATIONS

PSMA, prostate-specific membrane antigen; μPET, micropositron emission tomography; HSA, human serum albumin; mCRPC, metastasized castration-resistant prostate cancer; SCID, severe combined immunodeficiency; MIP, maximum intensity projection; TAC, time−activity curves; sst$_2$, somatostatin-2; PBS, phosphate buffered saline; HOAt, 1-hydroxy-7-azabenzotriazol; HATU, 1-[bis(dimethylamino)methylene]-1*H*-1,2,3-triazolo[4,5-*b*]pyridinium 3-oxid hexafluoro-phosphate; DIPEA, *N*,*N*-diisopropylethylamine; DMF, dimethylformamide; DCM, dichloromethane; HOBt, *N*-hydroxybenzotriazole; TBTU, *N*,*N*,*N*′,*N*′-tetramethyl-*O*-(benzotriazol-1-yl)-uronium tetrafluoroborate; Pd/C, palladium on activated charcoal; DIC, *N*,*N*′-diisopropylcarbodiimide; PfpOH, penta-fluorophenol; *t*Bu, *tert*-butyl; Fmoc, 9-fluorenylmethoxycarbonyl; 2-PMPA, 2-phosphonomethyl pentanedioic acid

REFERENCES

(1) Ghosh, A.; Heston, W. D. W. Tumor target prostate specific membrane antigen (PSMA) and its regulation in prostate cancer. *J. Cell. Biochem.* **2004**, *91*, 528−539.

(2) Ross, J. S.; Sheehan, C. E.; Fisher, H. A.; Kaufman, R. P.; Kaur, P.; Gray, K.; Webb, I.; Gray, G. S.; Mosher, R.; Kallakury, B. V. Correlation of primary tumor prostate-specific membrane antigen expression with disease recurrence in prostate cancer. *Clin. Cancer Res.* **2003**, *9*, 6357−6362.

(3) Smith-Jones, P. M.; Vallabahajosula, S.; Goldsmith, S. J.; Navarro, V.; Hunter, C. J.; Bastidas, D.; Bander, N. H. In vitro characterization of radiolabeled monoclonal antibodies specific for the extracellular domain of prostate-specific membrane antigen. *Cancer Res.* **2000**, *60*, 5237−5243.

(4) Horoszewicz, J. S.; Kawinski, E.; Murphy, G. Monoclonal antibodies to a new antigenic marker in epithelial prostatic cells and serum of prostatic cancer patients. *Anticancer Res.* **1987**, *7*, 927−935.

(5) Eder, M.; Schäfer, M.; Bauder-Wüst, U.; Hull, W.-E.; Wängler, C.; Mier, W.; Haberkorn, U.; Eisenhut, M. 68Ga-complex lipophilicity and the targeting property of a urea-based PSMA inhibitor for PET imaging. *Bioconjugate Chem.* **2012**, *23*, 688−697.

(6) Benešová, M.; Schäfer, M.; Bauder-Wüst, U.; Afshar-Oromieh, A.; Kratochwil, C.; Mier, W.; Haberkorn, U.; Kopka, K.; Eder, M. Preclinical Evaluation of a Tailor-Made DOTA-Conjugated PSMA Inhibitor with Optimized Linker Moiety for Imaging and Endoradiotherapy of Prostate Cancer. *J. Nucl. Med.* **2015**, *56*, 914−920.

(7) Weineisen, M.; Schottelius, M.; Simecek, J.; Eiber, M.; Schwaiger, M.; Wester, H. Development and first in human evaluation of PSMA I&T-A ligand for diagnostic imaging and endoradiotherapy of prostate cancer. *J. Nucl. Med.* **2014**, *55*, 1083.

(8) Barrett, J. A.; Coleman, R. E.; Goldsmith, S. J.; Vallabhajosula, S.; Petry, N. A.; Cho, S.; Armor, T.; Stubbs, J. B.; Maresca, K. P.; Stabin, M. G.; Joyal, J. L.; Eckelman, W. C.; Babich, J. W. First-in-man evaluation of 2 high-affinity PSMA-avid small molecules for imaging prostate cancer. *J. Nucl. Med.* **2013**, *54*, 380−387.

(9) Smith-Jones, P. M.; Vallabhajosula, S.; Navarro, V.; Bastidas, D.; Goldsmith, S. J.; Bander, N. H. Radiolabeled monoclonal antibodies specific to the extracellular domain of prostate-specific membrane antigen: preclinical studies in nude mice bearing LNCaP human prostate tumor. *Urol. Oncol.: Semin. Orig. Invest.* **2003**, *21*, 486.

(10) Chen, Y.; Pullambhatla, M.; Foss, C. A.; Byun, Y.; Nimmagadda, S.; Senthamizhchelvan, S.; Sgouros, G.; Mease, R. C.; Pomper, M. G. 2-(3- -Ureido)-Pentanedioic Acid, [18F]DCFPyL, a PSMA-Based PET Imaging Agent for Prostate Cancer. *Clin. Cancer Res.* **2011**, *17*, 7645−7653.

(11) Chen, Y.; Foss, C. A.; Byun, Y.; Nimmagadda, S.; Pullambhatla, M.; Fox, J. J.; Castanares, M.; Lupold, S. E.; Babich, J. W.; Mease, R. C.; Pomper, M. G. Radiohalogenated prostate-specific membrane antigen (PSMA)-based ureas as imaging agents for prostate cancer. *J. Med. Chem.* **2008**, *51*, 7933−7943.

(12) Baum, R. P.; Kulkarni, H. R.; Schuchardt, C.; Singh, A.; Wirtz, M.; Wiessalla, S.; Schottelius, M.; Mueller, D.; Klette, I.; Wester, H.-J. 177Lu-labeled prostate-specific membrane antigen radioligand therapy of metastatic castration-resistant prostate cancer: safety and efficacy. *J. Nucl. Med.* **2016**, *57*, 1006−1013.

(13) Kulkarni, H. R.; Singh, A.; Schuchardt, C.; Niepsch, K.; Sayeg, M.; Leshch, Y.; Wester, H.-J.; Baum, R. P. PSMA-Based Radioligand Therapy for Metastatic Castration-Resistant Prostate Cancer: The Bad Berka Experience Since 2013. *J. Nucl. Med.* **2016**, *57*, 97S−104S.

(14) Baum, R. P.; Kulkarni, H. R.; Schuchardt, C.; Singh, A.; Wirtz, M.; Wiessalla, S.; Schottelius, M.; Mueller, D.; Klette, I.; Wester, H.-J. Lutetium-177 PSMA radioligand therapy of metastatic castration-resistant prostate cancer: safety and efficacy. *J. Nucl. Med.* **2016**, *57*, 1006.

(15) Kratochwil, C.; Bruchertseifer, F.; Giesel, F. L.; Weis, M.; Verburg, F. A.; Mottaghy, F.; Kopka, K.; Apostolidis, C.; Haberkorn,

U.; Morgenstern, A. 225Ac-PSMA-617 for PSMA targeting alpha-radiation therapy of patients with metastatic castration-resistant prostate cancer. *J. Nucl. Med.* **2016**, *57*, 1941.

(16) Wester, H.; Schottelius, M.; Scheidhauer, K.; Meisetschläger, G.; Herz, M.; Rau, F.; Reubi, J.; Schwaiger, M. PET imaging of somatostatin receptors: design, synthesis and preclinical evaluation of a novel 18 F-labelled, carbohydrated analogue of octreotide. *Eur. J. Nucl. Med. Mol. Imaging* **2003**, *30*, 117−122.

(17) Schottelius, M.; Wester, H.-J.; Reubi, J. C.; Senekowitsch-Schmidtke, R.; Schwaiger, M. Improvement of pharmacokinetics of radioiodinated Tyr3-octreotide by conjugation with carbohydrates. *Bioconjugate Chem.* **2002**, *13*, 1021−1030.

(18) Wester, H.-J.; Schottelius, M.; Scheidhauer, K.; Reubi, J.-C.; Wolf, I.; Schwaiger, M. Comparison of radioiodinated TOC, TOCA and Mtr-TOCA: the effect of carbohydration on the pharmacokinetics. *Eur. J. Nucl. Med. Mol. Imaging* **2002**, *29*, 28−38.

(19) Schottelius, M.; Rau, F.; Reubi, J. C.; Schwaiger, M.; Wester, H.-J. Modulation of pharmacokinetics of radioiodinated sugar-conjugated somatostatin analogues by variation of peptide net charge and carbohydration chemistry. *Bioconjugate Chem.* **2005**, *16*, 429−437.

(20) Weineisen, M.; Simecek, J.; Schottelius, M.; Schwaiger, M.; Wester, H.-J. Synthesis and preclinical evaluation of DOTAGA-conjugated PSMA ligands for functional imaging and endoradiotherapy of prostate cancer. *EJNMMI Res.* **2014**, *4*, 63.

(21) Sosabowski, J. K.; Mather, S. J. Conjugation of DOTA-like chelating agents to peptides and radiolabeling with trivalent metallic isotopes. *Nat. Protoc.* **2006**, *1*, 972−976.

(22) Maresca, K. P.; Hillier, S. M.; Femia, F. J.; Keith, D.; Barone, C.; Joyal, J. L.; Zimmerman, C. N.; Kozikowski, A. P.; Barrett, J. A.; Eckelman, W. C. A series of halogenated heterodimeric inhibitors of prostate specific membrane antigen (PSMA) as radiolabeled probes for targeting prostate cancer. *J. Med. Chem.* **2009**, *52*, 347−357.

(23) Vaidyanathan, G.; Zalutsky, M. R. Preparation of N-succinimidyl 3-[*I]iodobenzoate: an agent for the indirect radioiodination of proteins. *Nat. Protoc.* **2006**, *1*, 707−713.

(24) Dekker, B.; Keen, H.; Shaw, D.; Disley, L.; Hastings, D.; Hadfield, J.; Reader, A.; Allan, D.; Julyan, P.; Watson, A.; Zweit, J. Functional comparison of annexin V analogues labeled indirectly and directly with iodine-124. *Nucl. Med. Biol.* **2005**, *32*, 403−413.

(25) Valko, K.; Nunhuck, S.; Bevan, C.; Abraham, M. H.; Reynolds, D. P. Fast gradient HPLC method to determine compounds binding to human serum albumin. Relationships with octanol/water and immobilized artificial membrane lipophilicity. *J. Pharm. Sci.* **2003**, *92*, 2236−2248.

(26) Yamazaki, K.; Kanaoka, M. Computational prediction of the plasma protein-binding percent of diverse pharmaceutical compounds. *J. Pharm. Sci.* **2004**, *93*, 1480−1494.

(27) Robu, S.; Schottelius, M.; Eiber, M.; Maurer, T.; Gschwend, J.; Schwaiger, M.; Wester, H.-J. Preclinical evaluation and first patient application of 99mTc-PSMA-I&S for SPECT imaging and radio-guided surgery in prostate cancer. *J. Nucl. Med.* **2016**, *58*, 235.

(28) Afshar-Oromieh, A.; Avtzi, E.; Giesel, F. L.; Holland-Letz, T.; Linhart, H. G.; Eder, M.; Eisenhut, M.; Boxler, S.; Hadaschik, B. A.; Kratochwil, C.; Weichert, W.; Kopka, K.; Debus, J.; Haberkorn, U. The diagnostic value of PET/CT imaging with the 68Ga-labelled PSMA ligand HBED-CC in the diagnosis of recurrent prostate cancer. *Eur. J. Nucl. Med. Mol. Imaging* **2015**, *42*, 197−209.

(29) Szabo, Z.; Mena, E.; Rowe, S. P.; Plyku, D.; Nidal, R.; Eisenberger, M. A.; Antonarakis, E. S.; Fan, H.; Dannals, R. F.; Chen, Y.; Mease, R. C.; Vranesic, M.; Bhatnagar, A.; Sgouros, G.; Cho, S. Y.; Pomper, M. G. Initial Evaluation of [18F]DCFPyL for Prostate-Specific Membrane Antigen (PSMA)-Targeted PET Imaging of Prostate Cancer. *Mol. Imaging Biol.* **2015**, *17*, 565−574.

(30) Hillier, S. M.; Maresca, K. P.; Femia, F. J.; Marquis, J. C.; Foss, C. A.; Nguyen, N.; Zimmerman, C. N.; Barrett, J. A.; Eckelman, W. C.; Pomper, M. G.; Joyal, J. L.; Babich, J. W. Preclinical evaluation of novel glutamate-urea-lysine analogues that target prostate-specific

membrane antigen as molecular imaging pharmaceuticals for prostate cancer. *Cancer Res.* **2009**, *69*, 6932−6940.

(31) Bander, N. H.; Trabulsi, E. J.; Kostakoglu, L.; Yao, D.; Vallabhajosula, S.; Smith-Jones, P.; Joyce, M. A.; Milowsky, M.; Nanus, D. M.; Goldsmith, S. J. Targeting metastatic prostate cancer with radiolabeled monoclonal antibody J591 to the extracellular domain of prostate specific membrane antigen. *J. Urol.* **2003**, *170*, 1717−1721.

(32) Eiber, M.; Heck, M.; Tauber, R.; Rauscher, I.; Calogero, D.; Maurer, T.; Retz, M.; Wester, H.; Schwaiger, M. Systemic radioligand therapy with 177Lu-PSMA I&T in patients with metastatic castration-resistant prostate cancer. *J. Nucl. Med.* **2016**, *57*, 61.

(33) Schottelius, M.; Reubi, J. C.; Eltschinger, V.; Schwaiger, M.; Wester, H.-J. N-Terminal Sugar Conjugation and C-Terminal Thr-for-Thr(ol) Exchange in Radioiodinated Tyr3-octreotide: Effect on Cellular Ligand Trafficking in Vitro and Tumor Accumulation in Vivo. *J. Med. Chem.* **2005**, *48*, 2778−2789.

(34) Suzuki, K.; Susaki, H.; Okuno, S.; Yamada, H.; Watanabe, H. K.; Sugiyama, Y. Specific renal delivery of sugar-modified low-molecular-weight peptides. *J. Pharmacol. Exp. Ther.* **1999**, *288*, 888−897.

(35) Haubner, R.; Wester, H.-J.; Burkhart, F.; Senekowitsch-Schmidtke, R.; Weber, W.; Goodman, S. L.; Kessler, H.; Schwaiger, M. Glycosylated RGD-containing peptides: tracer for tumor targeting and angiogenesis imaging with improved biokinetics. *J. Nucl. Med.* **2001**, *42*, 326−336.

(36) Haubner, R.; Weber, W. A.; Beer, A. J.; Vabuliene, E.; Reim, D.; Sarbia, M.; Becker, K.-F.; Goebel, M.; Hein, R.; Wester, H.-J.; Kessler, H.; Schwaiger, M. Noninvasive Visualization of the Activated αvβ3 Integrin in Cancer Patients by Positron Emission Tomography and [18F]Galacto-RGD. *PLoS Med.* **2005**, *2*, No. e70.

(37) Richter, S.; Wuest, M.; Bergman, C. N.; Way, J. D.; Krieger, S.; Rogers, B. E.; Wuest, F. Rerouting the metabolic pathway of 18F-labeled peptides: the influence of prosthetic groups. *Bioconjugate Chem.* **2015**, *26*, 201−212.

(38) Suzuki, K.; Susaki, H.; Okuno, S.; Sugiyama, Y. Renal drug targeting using a vector "alkylglycoside". *J. Pharmacol. Exp. Ther.* **1999**, *288*, 57−64.

(39) Susaki, H.; Suzuki, K.; Yamada, H.; Okuno, S.; Watanabe, H. K. Renal targeting of arginine-vasopressin by modification with carbohydrates at the tyrosine side chain. *Biol. Pharm. Bull.* **1999**, *22*, 1094−1098.

(40) Bouvet, V.; Wuest, M.; Bailey, J. J.; Bergman, C.; Janzen, N.; Valliant, J. F.; Wuest, F. Targeting Prostate-Specific Membrane Antigen (PSMA) with F-18-Labeled Compounds: the Influence of Prosthetic Groups on Tumor Uptake and Clearance Profile. *Mol. Imaging Biol.* **2017**, *19*, 923−932.

(41) Davis, M. I.; Bennett, M. J.; Thomas, L. M.; Bjorkman, P. J. Crystal structure of prostate-specific membrane antigen, a tumor marker and peptidase. *Proc. Natl. Acad. Sci. U.S.A.* **2005**, *102*, 5981−5986.

(42) Barinka, C.; Byun, Y.; Dusich, C. L.; Banerjee, S. R.; Chen, Y.; Castanares, M.; Kozikowski, A. P.; Mease, R. C.; Pomper, M. G.; Lubkowski, J. Interactions between Human Glutamate Carboxypeptidase II and Urea-Based Inhibitors: Structural Characterization†. *J. Med. Chem.* **2008**, *51*, 7737−7743.

(43) Barinka, C.; Hlouchova, K.; Rovenska, M.; Majer, P.; Dauter, M.; Hin, N.; Ko, Y.-S.; Tsukamoto, T.; Slusher, B. S.; Konvalinka, J.; Lubkowski, J. Structural basis of interactions between human glutamate carboxypeptidase II and its substrate analogs. *J. Mol. Biol.* **2008**, *376*, 1438−1450.

(44) Wüstemann, T.; Bauder-Wüst, U.; Schäfer, M.; Eder, M.; Benesova, M.; Leotta, K.; Kratochwil, C.; Haberkorn, U.; Kopka, K.; Mier, W. Design of Internalizing PSMA-specific Glu-ureido-based Radiotherapeuticals. *Theranostics* **2016**, *6*, 1085−1095.

(45) Liu, H.; Rajasekaran, A. K.; Moy, P.; Xia, Y.; Kim, S.; Navarro, V.; Rahmati, R.; Bander, N. H. Constitutive and antibody-induced internalization of prostate-specific membrane antigen. *Cancer Res.* **1998**, *58*, 4055−4060.

(46) Liu, T.; Toriyabe, Y.; Kazak, M.; Berkman, C. E. Pseudoirreversible Inhibition of Prostate-Specific Membrane Antigen by Phosphoramidate Peptidomimetics†. *Biochemistry* **2008**, *47*, 12658−12660.

(47) Muller, C.; Struthers, H.; Winiger, C.; Zhernosekov, K.; Schibli, R. DOTA Conjugate with an Albumin-Binding Entity Enables the First Folic Acid-Targeted 177Lu-Radionuclide Tumor Therapy in Mice. *J. Nucl. Med.* **2013**, *54*, 124−131.

(48) Choy, C. J.; Ling, X.; Geruntho, J. J.; Beyer, S. K.; Latoche, J. D.; Langton-Webster, B.; Anderson, C. J.; Berkman, C. E. 177Lu-Labeled Phosphoramidate-Based PSMA Inhibitors: The Effect of an Albumin Binder on Biodistribution and Therapeutic Efficacy in Prostate Tumor-Bearing Mice. *Theranostics* **2017**, *7*, 1928.

(49) Kelly, J. M.; Amor-Coarasa, A.; Nikolopoulou, A.; Wüstemann, T.; Barelli, P.; Kim, D.; Williams, C.; Zheng, X.; Bi, C.; Hu, B.; Warren, J. D.; Hage, D. S.; DiMagno, S. G.; Babich, J. W. Dual-Target Binding Ligands with Modulated Pharmacokinetics for Endoradiotherapy of Prostate Cancer. *J. Nucl. Med.* **2017**, *58*, 1442−1449.

(50) Tucker, G. T. Measurement of the renal clearance of drugs. *Br. J. Clin. Pharmacol.* **1981**, *12*, 761−770.

(51) Benešová, M.; Umbricht, C. A.; Schibli, R.; Müller, C. Albumin-binding PSMA ligands: optimization of the tissue distribution profile. *Mol. Pharmaceutics* **2018**, *15*, 934−946.

(52) Weineisen, M.; Schottelius, M.; Simecek, J.; Baum, R. P.; Yildiz, A.; Beykan, S.; Kulkarni, H. R.; Lassmann, M.; Klette, I.; Eiber, M.; Schwaiger, M.; Wester, H.-J. 68Ga- and 177Lu-Labeled PSMA I&T: Optimization of a PSMA-Targeted Theranostic Concept and First Proof-of-Concept Human Studies. *J. Nucl. Med.* **2015**, *56*, 1169−1176.

(53) Benesova, M.; Bauder-Wüst, U.; Schäfer, M.; Klika, K. D.; Mier, W.; Haberkorn, U.; Kopka, K.; Eder, M. Linker Modification Strategies To Control the Prostate-Specific Membrane Antigen (PSMA)-Targeting and Pharmacokinetic Properties of DOTA-Conjugated PSMA Inhibitors. *J. Med. Chem.* **2016**, *59*, 1761−1775.

(54) Ginj, M.; Zhang, H.; Waser, B.; Cescato, R.; Wild, D.; Wang, X.; Erchegyi, J.; Rivier, J.; Macke, H. R.; Reubi, J. C. Radiolabeled somatostatin receptor antagonists are preferable to agonists for in vivo peptide receptor targeting of tumors. *Proc. Natl. Acad. Sci. U.S.A.* **2006**, *103*, 16436−16441.

(55) Cescato, R.; Maina, T.; Nock, B.; Nikolopoulou, A.; Charalambidis, D.; Piccand, V.; Reubi, J. C. Bombesin receptor antagonists may be preferable to agonists for tumor targeting. *J. Nucl. Med.* **2008**, *49*, 318−326.

(56) Wild, D.; Fani, M.; Fischer, R.; Del Pozzo, L.; Kaul, F.; Krebs, S.; Fischer, R.; Rivier, J. E. F.; Reubi, J. C.; Maecke, H. R.; Weber, W. A. Comparison of somatostatin receptor agonist and antagonist for peptide receptor radionuclide therapy: a pilot study. *J. Nucl. Med.* **2014**, *55*, 1248−1252.

(57) Rylova, S. N.; Waser, B.; Del Pozzo, L.; Tonnesmann, R.; Mansi, R.; Meyer, P. T.; Reubi, J. C.; Maecke, H. R. Approaches to improve the pharmacokinetics of radiolabeled glucagon-like peptide-1 receptor ligands using antagonistic tracers. *J. Nucl. Med.* **2016**, *57*, 1282−1288.

(58) Notni, J.; Šimeček, J.; Hermann, P.; Wester, H.-J. TRAP, a Powerful and Versatile Framework for Gallium-68 Radiopharmaceuticals. *Chem.—Eur. J.* **2011**, *17*, 14718−14722.

(59) Notni, J.; Pohle, K.; Wester, H.-J. Comparative gallium-68 labeling of TRAP-, NOTA-, and DOTA-peptides: practical consequences for the future of gallium-68-PET. *EJNMMI Res.* **2012**, *2*, 28.